3073

NACA TN 2707

TECH LIBRARY KAFB, NM
0065767

NATIONAL ADVISORY COMMITTEE FOR AERONAUTICS

TECHNICAL NOTE 2707

ANALOGUE-COMPUTER SIMULATION OF AN AUTOPILOT SERVO SYSTEM HAVING NONLINEAR RESPONSE CHARACTERISTICS

By Arthur L. Jones and John S. White

Ames Aeronautical Laboratory
Moffett Field, Calif.

Washington
June 1952

AFMDC
TECHNICAL LIBRARY
AFL 2811

TECH LIBRARY KAFB, NM
0065767

V

NATIONAL ADVISORY COMMITTEE FOR AERONAUTICS

TECHNICAL NOTE 2707

ANALOGUE-COMPUTER SIMULATION OF AN AUTOPILOT SERVO SYSTEM HAVING NONLINEAR RESPONSE CHARACTERISTICS

By Arthur L. Jones and John S. White

SUMMARY

The nonlinear response characteristics of an electrohydraulic servo system were successfully simulated using an electronic analogue computer (differential analyzer). This servo system was the control unit of an autopilot used in the automatic stabilization and control of an aircraft. One element of the servo system, the amplifier, tended to saturate beyond certain voltage input magnitudes and was the cause of the nonlinear response. In obtaining a satisfactory simulation of the servo system it was necessary not only to take into account the nonlinear amplifier characteristics but also the accumulative effect of some time lags of the servo system.

INTRODUCTION

The analysis or synthesis of a system having a dynamic response is simplified if the system can be considered to be linear rather than nonlinear. Such systems are readily amenable to mathematical solution and the effects of a large number of parameter changes can be studied separately, due to the property of superposition that exists for solutions of linear differential equations. For various reasons, automatic guidance systems for aircraft often contain elements that have nonlinear responses during certain phases of their operation. Depending upon the degree of these nonlinearities, the system may respond in a fairly linear manner and therefore be amenable to a linear analysis, or it may be necessary to consider the system as one having definitely nonlinear characteristics. The servo system considered in this report is in the latter category, due mainly to the fact that its amplifier tends to saturate.

This particular servo system was part of an autopilot used to stabilize the longitudinal motion of a dive-bomber type of aircraft. It constituted the control unit required to convert a pitch angle and pitch-rate signal from the autopilot sensing devices into a deflection of the

aircraft elevator control. An investigation of the longitudinal dynamic response of the stabilized airplane was made and the results were reported in reference 1. In this investigation it was found that when restricted to linear methods of analysis the performance of the autopilot-aircraft combination could be predicted for only the small range of operation where the elements of the autopilot operated within their linear range. Consequently, in order to study the gross effects of the autopilot on the performance of the stabilized airplane it would be necessary either to test the equipment extensively in flight or to develop a way of readily simulating the operational characteristics of the nonlinear autopilot. If the latter is possible it is reasonable to assume that the operational characteristics of the aircraft could also be simulated; thus it seems that simulation would be the most expedient way to determine the effects of the autopilot on the characteristics of the combination.

In this investigation an analogue computer, in particular, the Reeves Electronic Analogue Computer, was used as the means for simulation. A machine of this type furnishes a rapid solution to ordinary nonlinear differential equations of the degree of complexity generally encountered in fairly simple mechanical or electrical systems. Consequently, an analogue machine is a convenient means for handling nonlinear problems of this type.

NOTATION

A_m transfer function of the actuator, inches per milliampere

f frequency, cycles per second

I current from amplifier, milliamperes

k closed-loop transfer-function constant, per second squared

k_f follow-up selsyn constant, volts per inch

k_g displacement gyro constant, volts per degree

k_m actuator transfer-function constant, inches per second-milliampere

M_p peak amplitude on frequency response curve

P_aA_a static gain constant of amplifier, milliamperes per volt

P_f gain of sensitivity potentiometer, percent

P_rA_r transfer function of rate gyro, volt-seconds per degree

R amplitude ratio of closed-loop servo response

s variable introduced in the Laplace transformation, per second

t time, seconds

v_E error signal of autopilot-aircraft combination $(v_I - v_g)$, volts

v_e error signal of servo system $(v_i - v_f)$, volts

v_f feedback voltage of servo system, volts

v_g displacement gyro output, volts

v_I input signal to autopilot-aircraft combination, volts

v_i input signal to servo system, volts

v_r rate gyro output, volts

δ control-surface deflection measured in terms of servo output shaft, inches

ϵ_e phase angle of v_e relative to v_i, degrees

ϵ_f phase angle of v_f relative to v_i, degrees

ζ damping ratio of servo system

θ_I input angle to autopilot-aircraft combination, degrees

θ_i hypothetical input angle to servo system, degrees

θ_o attitude of aircraft in angular displacement, degrees

τ_D time delay constant, seconds

τ_m time constant of actuator, seconds

φ phase angle by which the measured open-loop response differs from the response of the second-order term $\left[\frac{1}{s(1+\tau_m s)}\right]$, degrees

ω_n natural frequency of servo systems, radians per second

ω_p frequency at peak amplitude of frequency response curve, radians per second

DESCRIPTION OF SERVO SYSTEM

The servo system under consideration is part of an autopilot that provides longitudinal stability for an aircraft. As shown by the block diagram (fig. 1) the stabilizing action is produced by comparing the desired pitch angle θ_I with the instantaneous pitch angle θ_o, which is measured by a gyroscope. An error signal $v_E = v_I - v_g$ in volts, which is directly proportional to the difference between θ_I and θ_o, and a signal v_r which is proportional to the rate of change of the output pitch angle $d\theta_o/dt$ are combined to form the input signal v_i to the servo system. In the servo system the signal is amplified and then by means of a solenoid-controlled transfer valve which operates a hydraulic piston the signal is used to control the elevator deflection δ. The purpose of the internal feedback loop which compares v_f to v_i, the difference being v_e, is to provide zero static error for the servo system. The net effects of the afore-mentioned displacement signal $\theta_I - \theta_o$ and rate signal $d\theta_o/dt$ on the combined aircraft-autopilot system could be considered as increases in the restoring force and in the damping of the system, respectively.

The characteristics of the elements that make up the servo system were determined by laboratory bench tests. The amplifier, which was the critical element with respect to linearity, had a constant static gain of $P_aA_a = 120$ milliamperes per volt up to an input voltage of approximately ±0.35 volt. At that point its response tended to deviate from the linear as shown in figure 2, and above approximately ±0.65 volt input the amplifier was completely saturated, giving about 53 milliamperes output. It was reasonably assumed that the dynamic characteristics of the amplifier did not differ appreciably from the static characteristics. If minor differences did exist, however, they were absorbed into the transfer function representing the actuator, due to the fact that such differences would show up in the closed-loop response measurements used in determining the actuator transfer function. The other elements having static gains were the follow-up selsyn attached to the servo output shaft for which $k_f = 12.8$ volts per inch, and the sensitivity potentiometer P_f which could be set to vary the follow-up-selsyn output anywhere from 0 to 100 percent. The experimental data obtained for this analysis were for sensitivities of $P_f = 0.24$, 0.33, 0.42, 0.52, and 0.63.

The actuator consisted of a hydraulic piston operated by a solenoid-controlled transfer valve. In previous closed-loop measurements it was determined that the dynamic response characteristics of the actuator could be represented by a transfer function of the following form:[1]

$$A_m(s) = \frac{\delta}{I}(s) = \frac{k_m}{s(1+\tau_m s)} \text{ inches/milliampere} \tag{1}$$

The constant k_m is frequency invariant and is readily determinable from open-loop tests of the forward branch of the servo loop shown below.

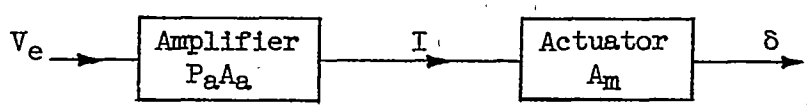

Measurements of the rate of the actuator piston travel in inches per second made within the linear range of amplifier operation were divided by the voltage input v_e giving a value of 7.6 inches per second per volt. Then by dividing out the amplifier constant P_aA_a the constant k_m was obtained as

$$k_m = \frac{7.6}{120} = 0.063 \text{ in./sec-ma}$$

The time constant τ_m is hard to measure directly. It is possible to determine it, however, from open-loop frequency-response measurements, $\frac{\delta}{v_e}(i\omega)$, or from closed-loop frequency-response measurements, $\frac{\delta}{v_i}(j\omega)$, provided that the response is that of a linear second-order system. In making the measurements required to determine this constant, therefore, it is necessary to restrict the input signals to a magnitude small enough to prevent the amplifier from saturating. The closed-loop frequency responses were used to this end inasmuch as they had already been obtained for final checking of the simulated response characteristics and contained a number of measurements for which the amplifier operation was linear. These linear responses represented the frequency-response characteristics of the following second-order system:

$$\frac{\delta}{v_i}(s) = \frac{P_aA_a\ A_m(s)}{1 + P_aA_a\ P_f\ k_f\ A_m(s)} \text{ inches per volt} \tag{2}$$

[1]The operational notation used herein corresponds to the Laplacian notation used by Churchill in reference 2.

or

$$\frac{\delta}{v_i}(s) = \frac{P_a A_a\ k_m/s(1+\tau_m s)}{1 + P_a A_a\ P_f\ k_f\ k_m/s(1+\tau_m s)}$$

which can be written

$$\frac{\delta}{v_i}(s) = \frac{P_a A_a\ k_m/\tau_m}{s^2 + s/\tau_m + P_a A_a\ P_f\ k_f\ k_m/\tau_m} \tag{3}$$

The details of the procedure used to estimate the values of τ_m are given in a later section on analysis.

Since the follow-up voltage v_f is related to the deflection in the following manner

$$v_f = P_f\ k_f\ \delta$$

the closed-loop-response function can be written alternatively as

$$\frac{v_f}{v_i} = P_f\ k_f\ \frac{\delta}{v_i} \tag{4}$$

which becomes

$$\left.\begin{aligned} \frac{v_f}{v_i}(s) &= \frac{P_a A_a\ P_f\ k_f\ k_m/\tau_m}{s^2 + s/\tau_m + P_a A_a\ P_f\ k_f\ k_m/\tau_m} \\ \text{or} \qquad & \\ \frac{v_f}{v_i}(s) &= \frac{k}{s^2 + 2\zeta\omega_n s + \omega_n^2} \end{aligned}\right\} \tag{5}$$

where

$$\left.\begin{aligned} k &= P_a A_a\ P_f\ k_f\ k_m/\tau_m \\ 2\zeta\omega_n &= \frac{1}{\tau_m} \\ \omega_n^2 &= k = P_a A_a\ P_f\ k_f\ k_m/\tau_m \end{aligned}\right\} \tag{6}$$

The advantage of using this alternative form lies in the fact that it is dimensionless and that analytical results in this form can be compared directly with the bench-test results of the servo system which were obtained as dimensionless amplitude ratios.

ANALYSIS

Measured Response Characteristics of Servo System

In order to investigate the characteristics of the servo system over a wide operating range and thereby disclose the major effects of the nonlinear amplifier, closed-loop-response measurements were obtained for five different input voltages: $v_i = 0.1$, 0.2, 0.39, 0.78, and 1.56 volts; at each of three feedback sensitivities $P_f = 0.24$, 0.42, and 0.63; and also for $v_i = 0.1$ volt at $P_f = 0.33$ and 0.52. These results are presented in figure 3. The major effects noted were a decrease in both the peak amplitude and the frequency at peak amplitude with an increase in voltage input. A successful simulation of these characteristics over the wide range of variables investigated would be an indication that the method of simulation employed should be suitable for general dynamic studies of the aircraft-autopilot combination.

Simulation of Servo-System Characteristics

Although the REAC has been used mainly for solving linear differential equations, it can also be applied to solving nonlinear differential equations. Thus the REAC is a suitable instrument for simulating nonlinear mechanical or electrical systems. Other types of analogue computers can be used as simulators also.

On the REAC the nonlinear components can be included in the circuit representing the system by means of input tables, as was done in this case, or by generating the nonlinear function on the machine itself. The linear components in the circuit can be represented through the use of integrators, summers, and potentiometers.

As will be pointed out later, it was necessary to modify the originally assumed simulation system in order to obtain satisfactory simulation of the servo-system characteristics. Both the original and modified systems are described in the following paragraphs of this section.[2]

---

[2]Mr. Marvin Gore, formerly with the Ames Aeronautical Laboratory of the NACA, contributed to the development of these two simulation systems.

Second-order system incorporating nonlinear amplifier.- The representation of the servo system as originally assumed, that is, as shown in the block diagram of figure 1 and as represented by the transfer functions and constants given in the description of the servo system, is a second-order system incorporating a nonlinear function representing the amplifier. If the input voltage to the amplifier v_e is kept within the voltage range for which the amplifier responds in a linear fashion, the system, as visualized, is merely a linear second-order system. It is interesting to note that a great deal of information about the response of linear second-order systems is already known and catalogued and can be used to check the validity of the values determined for the constants as well as the validity of the assumed mathematical expression for the components. For this particular servo system, v_e must be kept smaller than 0.35 volt for the system to operate as a linear second-order system. This restriction can be expressed in terms of the closed-loop amplitude ratio and phase angle, R and ϵ_f, in the following manner:

Since

$$v_f = v_i \, Re^{j\epsilon_f}$$

where R is the closed-loop amplitude ratio and ϵ_f is the corresponding phase angle, then

$$\left.\begin{aligned} v_e = v_i - v_f &= v_i(1 - Re^{j\epsilon_f}) \\ &= v_i(1 - R\cos\epsilon_f - jR\sin\epsilon_f) \\ &= v_i\sqrt{1 + R^2 - 2R\cos\epsilon_f}\, e^{j\epsilon_e} \end{aligned}\right\} \tag{7}$$

and if the following relationship is maintained

$$\left|v_i\sqrt{1 + R^2 - 2R\cos\epsilon_f}\right| \leq 0.35 \tag{8}$$

the amplifier operates within its linear range. By use of this relationship and the closed-loop frequency-response curves shown in figure 3, it was determined that the amplifier had a linear response throughout the frequency spectrum for the voltage input of 0.1 and the feedback sensitivities of 0.24, 0.33, and 0.42. Furthermore, for the two higher feedback sensitivity values of 0.52 and 0.63, the responses for the voltage inputs of 0.1 indicated that, although the amplifier response deviated slightly from the linear for frequencies in the immediate vicinity of the resonant frequency, the amplifier was far from being fully saturated.

These linear responses of the closed-loop servo system were used to estimate a value of τ_m. It can be seen from equation (6) that for this second-order system τ_m is equal to the inverse of twice the product of the damping ratio ζ and the undamped natural frequency ω_n. Both of these factors can be obtained directly from the peak amplitude M_p and the frequency at peak amplitude ω_p of the frequency response. Thus, by means of equations (5) and (6) it is possible to write

$$\omega_n = \frac{\omega_p}{\sqrt{1 - 2\zeta^2}} \tag{9}$$

$$\zeta = \frac{1}{\sqrt{2}} \sqrt{1 - \sqrt{1 - (1/M_p^2)}} \tag{10}$$

and

$$\tau_m = \frac{1}{2\zeta\omega_n} = \frac{1}{\sqrt{2}\,\omega_p} \frac{\sqrt[4]{1 - (1/M_p^2)}}{\sqrt{1 - \sqrt{1 - (1/M_p^2)}}} \tag{11}$$

Substituting the values of M_p and ω_p from the responses to the five 0.1-volt-input cases into the above equation yielded

P_f	τ_m
0.24	0.071
.33	.074
.42	.084
.52	.083
.63	.094

The rather large variation in the values of τ_m obtained in this manner indicated that the system probably could not be adequately represented by the simple second-order system incorporating the nonlinear amplifier characteristics as initially assumed. A further check on this possibility was made by taking the value of τ_m for the feedback sensitivity of 0.24 and computing the linear response for a second-order system using the following constants:

$$\left.\begin{aligned} \tau_m &= 0.071 \\ k_m &= 0.063 \\ k_f &= 12.8 \\ P_aA_a &= 120 \end{aligned}\right\} \begin{array}{l} \text{estimated value} \\ \\ \text{measured values} \\ \\ \end{array}$$

This response is plotted for comparison with the servo system 0.1-volt-input response at this sensitivity in figure 4. The lack of agreement gave a further indication of the invalidity of the assumed representation of the servo system.

As a final check, the values of the two constants τ_m and k_m were adjusted to duplicate the servo-system response at 0.1 volt input ($\tau_m = 0.071$, $k_m = 0.076$). Then the assumed representation of the system including the nonlinear amplifier characteristic was put on the REAC and simulated responses were obtained for the voltage inputs 0.1, 0.39, and 1.56. These responses are compared with the actual system responses in figure 5. It is apparent from this comparison that although the simulated curves follow the same general trends of the actual responses, that is, a decrease in both the peak amplitude and the frequency at peak amplitude with an increase in voltage input, the matching of the curves is not close enough to make the simulation satisfactory.

Second-order system incorporating nonlinear amplifier and time-delay factor.- Various possible discrepancies in the originally assumed system representation were considered as sources of the inaccuracy in the simulation. No one component, however, could be identified as the probable source of the discrepancies. It was finally decided that a reasonable procedure would be to determine an average value of τ_m based on the assumption that the representation of the actuator was satisfactory, and to include, in addition, a time lag factor to take into account a series of time delays or lags that probably exist in one or more components in the main branch of the system. Such a procedure is suggested in reference 3 on pages 83 through 90. The appropriateness of including the lag factor was later confirmed by determining the difference in phase angles between the assumed second-order term $1/s(1+\tau_m s)$ and the open-loop phase-angle measurements of the main branch of the loop and comparing this difference with the phase lag that would be caused by a lag operator. The significance of this comparison is more fully explained in a later section of this report entitled "Discussion."

The average value of τ_m was selected on the basis that the variation of the natural frequency with the feedback sensitivity factor, for the 0.1-volt-input cases, was very close to what is predictable for this variation using the linear second-order representation of the servo system. In figure 6 the measured values of both ω_n and ζ are plotted against sensitivity on logarithmic scales and the corresponding theoretical linear variations are shown also. It is evident from this figure that whatever factor is preventing this system from behaving like a second-order system has had a greater effect on the damping ratio than on the natural frequency. It seems logical, therefore, to base the average value of τ_m on the measured values of ω_n which have been shown to correspond closely with the characteristics of a linear second-order

system. The following relationship, obtained from equation (6), was used

$$\tau_m = \frac{P_a A_a \; P_f \; k_f \; k_m}{\omega_n^2}$$

or

$$\tau_m = \frac{120(0.063)\; 12.8 \; P_f}{\omega_n^2} = \frac{96.7 \; P_f}{\omega_n^2}$$

which yielded the following results:

P_f	ω_n	τ_m
0.24	20.0	0.058
.33	24.8	.052
.42	28.3	.051
.52	32.4	.048
.63	35.4	.048

The average value of τ_m based on these calculations is 0.052.

Written in operational form for use as a transfer function the time lag factor can be expressed as $e^{-\tau_D s}$. This factor is often referred to as the lag operator. (See reference 4.) The constant τ_D represents a time delay in seconds which, in this case, can be thought of as an accumulated time delay in the main branch of the servo loop. The block diagram of the system would now appear as shown in figure 7. Since no measurement of such a time delay was available, an approximate value for τ_D was obtained by matching the response of the simulated system including the lag operator with the actual servo-response curves for a 0.1 volt input at the feedback sensitivity of 0.24. The value obtained in this manner was $\tau_D = 0.009$ second.

The simulated system was then set up on the REAC in order to check its suitability for the other voltage inputs and feedback sensitivities. The frequency response results obtained are shown in comparison with actual servo responses in figure 3. The matching of the curves, in general, is satisfactory. In particular nearly all of the curves match very well in the low-frequency ranges and on up to slightly beyond the frequency at peak amplitude. It appears, therefore, that a successful simulation of the servo system investigated can be obtained by the inclusion of the nonlinear amplifier characteristics and a lag operator in the linear second-order system originally assumed.

DISCUSSION

The results of the analysis showed that in order to simulate successfully the response of this electrohydraulic closed-loop servo system it was necessary to take into account time lags additional to those included in the originally assumed second-order system as well as to take into account the nonlinear amplifier characteristics. The degree of success of the simulation can be judged not only by the correspondence between the measured and simulated frequency responses of figure 3, but also by a comparison of the transient responses to a step input shown in figure 8 for feedback sensitivities of 0.24, 0.42, and 0.63 and input voltages of 0.1 and 0.78. In addition to the simulated response for the system incorporating the time lags and the nonlinear amplifier, a simulated response for a linear system without the time lags is shown for comparison. At the input voltage of 0.78 the linear simulation appears to be nearly as good as the nonlinear simulation for the sensitivities of 0.24 and 0.42. This apparent suitability of the linear simulation, however, would disappear as the input voltage increased because the amplifier saturation would become more effective, resulting in a reduction of the peak overshoots of both the measured and simulated nonlinear responses, while the peak overshoot of the linear response would be unaffected. All the transient responses of the simulated system incorporating the time lags and nonlinear amplifier correspond closely in initial overshoot and damping with those of the actual system. At the input voltages of 0.78 for the sensitivities of 0.42 and 0.63 there appears to be a slight shift in phase or a small difference in frequency or a combination of both these effects. The magnitudes of these differences, however, are small enough that they do not invalidate the success of the simulation to any appreciable degree.

The use of the lag operator to account for the difference between the originally assumed second-order system incorporating the nonlinear amplifier response and the actual response can be interpreted in two ways. As indicated previously, the lag operator can be used to take into account a number of time lags of either the exponential or dead-time type that may exist in the main branch of the servo loop. In this case no measurements of the individual time constants had been made so it was necessary to adjust the lag operator constant τ_D to fit the data for at least one frequency-response result. The fact that the value of this constant so determined was satisfactory when applied to calculating the responses for the other voltage inputs and sensitivities was, in effect, a confirmation of the practicability of using the lag operator in this manner. The other interpretation of the use of this lag operator is based on the fact that its effect can be very closely approximated by a first- or second-order term (depending on the size of τ_D) as shown by the following expansion formula:

$$e^{-\tau_D s} = \frac{1}{e^{\tau_D s}} = \frac{1}{1 + \tau_D s + \frac{(\tau_D s)^2}{2!} + \cdots + \frac{(\tau_D s)^n}{n!}}$$

In fact, in using the REAC it was necessary to approximate the lag factor in this manner. After it was found by computation that the value of τ_D should be 0.009 in order to fit the data, it was determined that the first three terms of the expansion, giving a second-order factor, would provide a very close approximation. The use of the lag operator therefore can be interpreted as an introduction of a linear factor of an order dependent on the magnitude of the time constant involved. In this case its use was equivalent to the introduction of a second-order factor, thereby raising the servo system to a fourth-order system.

At the conclusion of the analysis it was decided to make open-loop measurements of the main branch of the servo in order to obtain data from which at least the order of magnitude of the calculated time lag constant τ_D could be checked. In particular, the open-loop phase-angle measurements were employed in this check. By subtracting from these open-loop phase angles the phase angles corresponding to the acknowledged second-order term $1/s(1+\tau_m s)$ the phase angles contributed by the unaccounted for time lags could be determined. This difference in phase angles was then plotted against frequency as shown in figure 9. On this plot the time-lag factor can be identified as a phase lag versus frequency curve having a constant slope. It can be noted in figure 9 that, in spite of the scatter at low frequencies, the phase-angle curve corresponding to the unaccounted for time lags can be faired as a straight line having a slope of 3.4° per cycle per second. This corresponds to a time lag constant of $\tau_D = 0.0094$ second which very closely corresponds to the calculated value of 0.009 second.

CONCLUDING REMARKS

By using an electronic analogue computer it was possible to obtain a satisfactory simulation of a servo system having nonlinear response characteristics. The element of the servo system causing the nonlinear behavior was an amplifier. The characteristics of the amplifier were included in the analogue-computer circuit representing the system by means of an input table from which the nonlinear response of this element could be picked off and fed into the linearly responding elements simulated by the electronic integrating and summing components of the analogue computer. In addition, in order to achieve a successful simulation, it was necessary to take into account the accumulative effects of time lags in the servo which were not readily identifiable with the individual

components. Since the dynamic responses of an aircraft can also be simulated on an analogue computer, it is possible to conclude that the dynamic response of the combination, that is, the automatically controlled aircraft, could also be successfully simulated.

Ames Aeronautical Laboratory
National Advisory Committee for Aeronautics
Moffett Field, Calif., Mar. 11, 1952

REFERENCES

1. Smaus, Louis H., Gore, Marvin R., and Waugh, Merle G.: A Comparison of Predicted and Experimentally Determined Longitudinal Dynamic Responses of a Stabilized Airplane. NACA TN 2578, 1951.

2. Churchill, R. V.: Modern Operational Mathematics in Engineering. McGraw-Hill Book Company, Inc., New York, 1944.

3. Oldenbourg, R. C., and Sartorius, H.: The Dynamics of Automatic Controls. Trans. and ed. by H. L. Mason. American Soc. of Mech. Engrs., New York, 1948.

4. Jones, Arthur L., and Briggs, Benjamin R.: A Survey of Stability Analysis Techniques for Automatically Controlled Aircraft. NACA TN 2275, 1951.

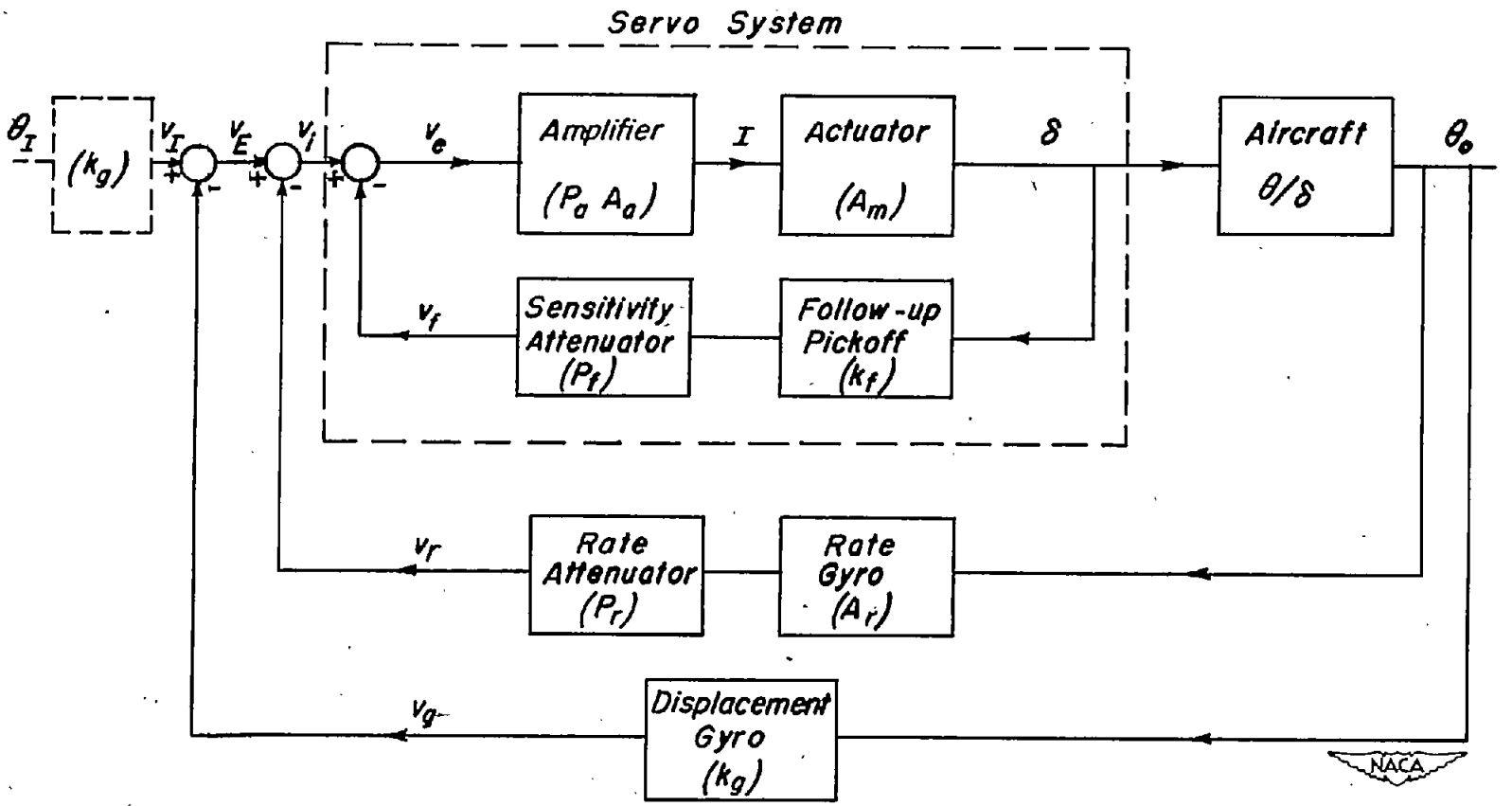

Figure 1.- Block diagram of autopilot-aircraft loop.

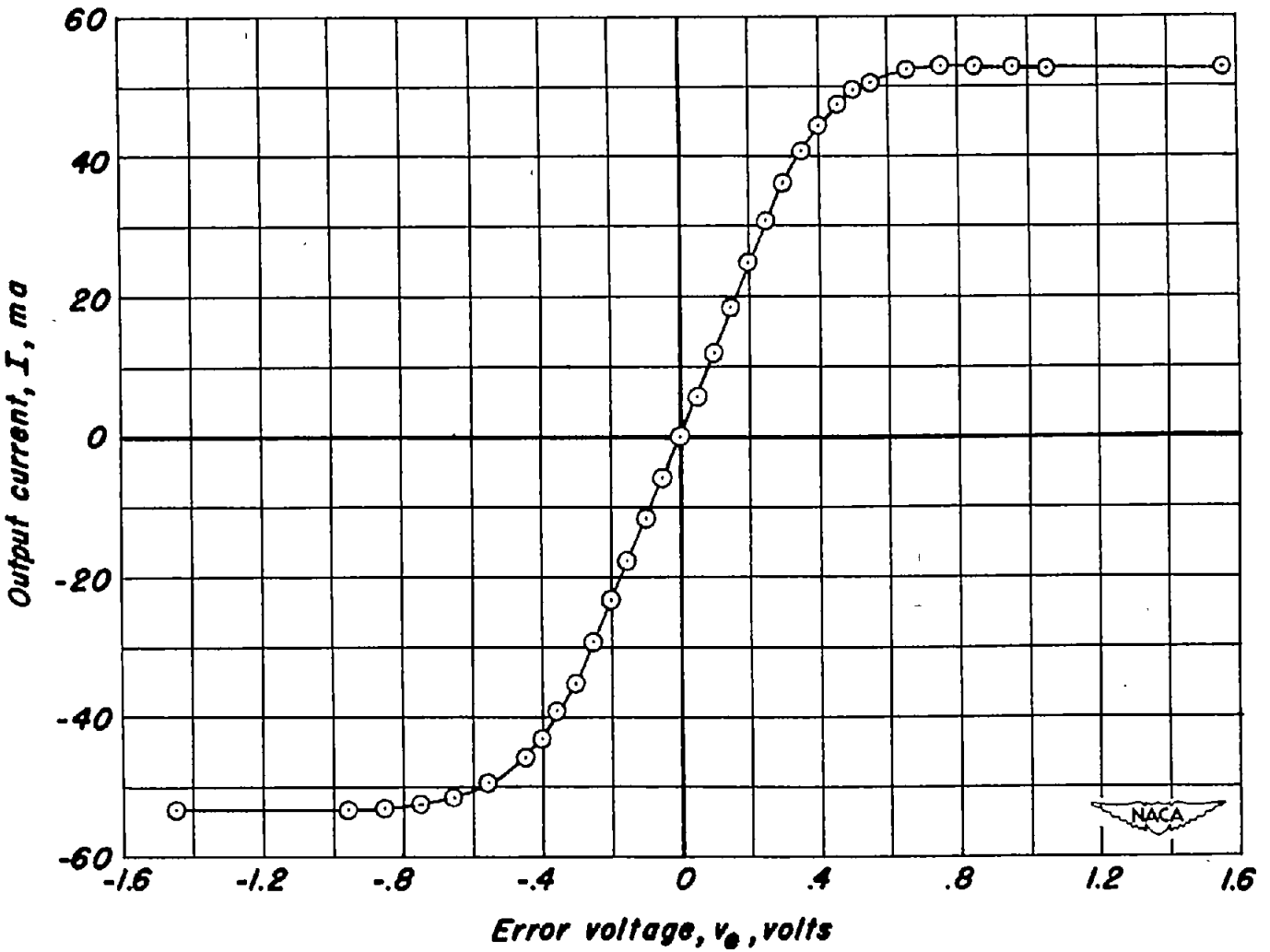

Figure 2.– Amplifier static response characteristics.

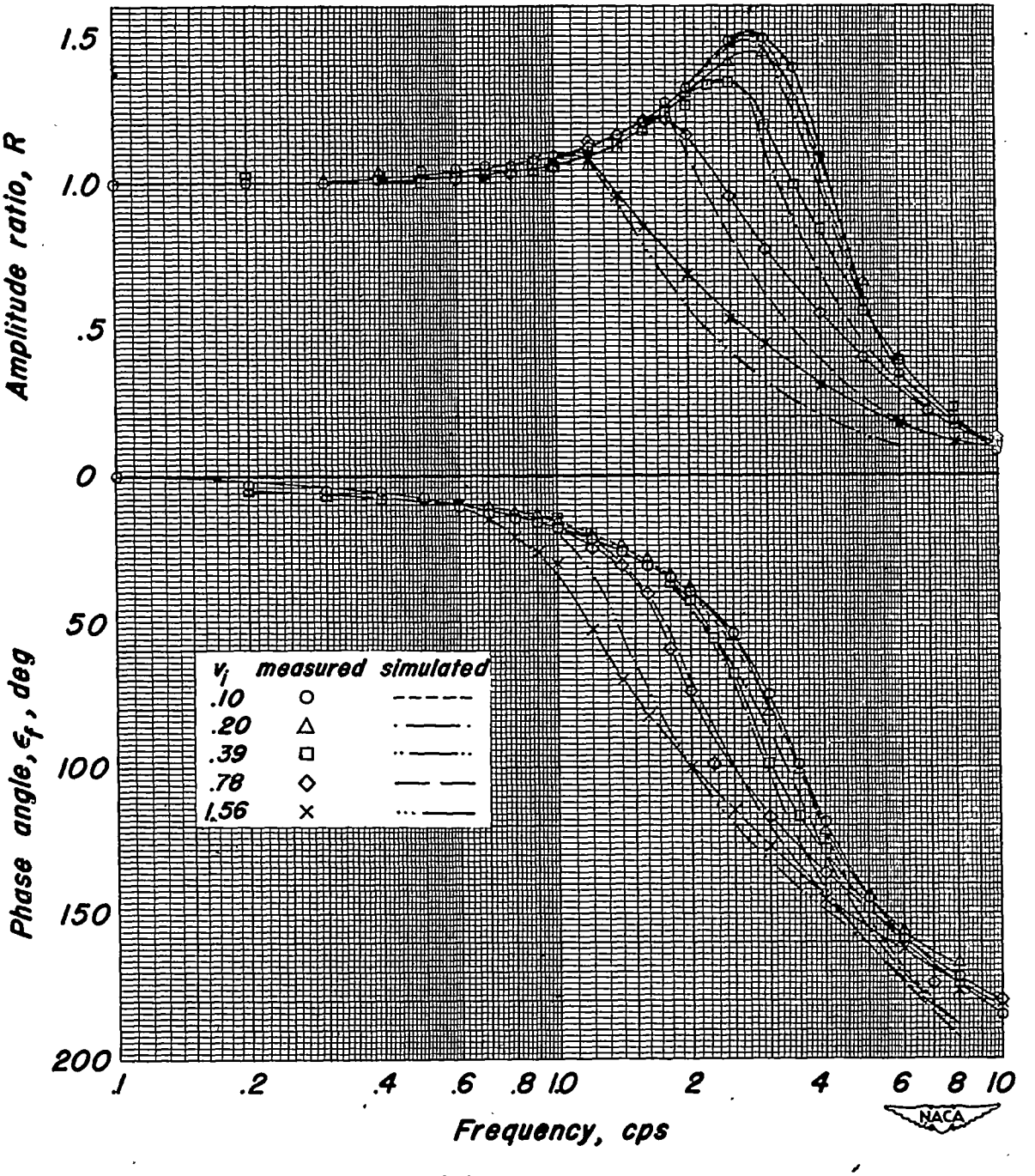

(a) $P_f = 0.24$

Figure 3.- Measured and simulated closed-loop frequency responses of servo system. For simulation $k_m = 0.063$, $\tau_m = 0.052$, $\tau_D = 0.009$.

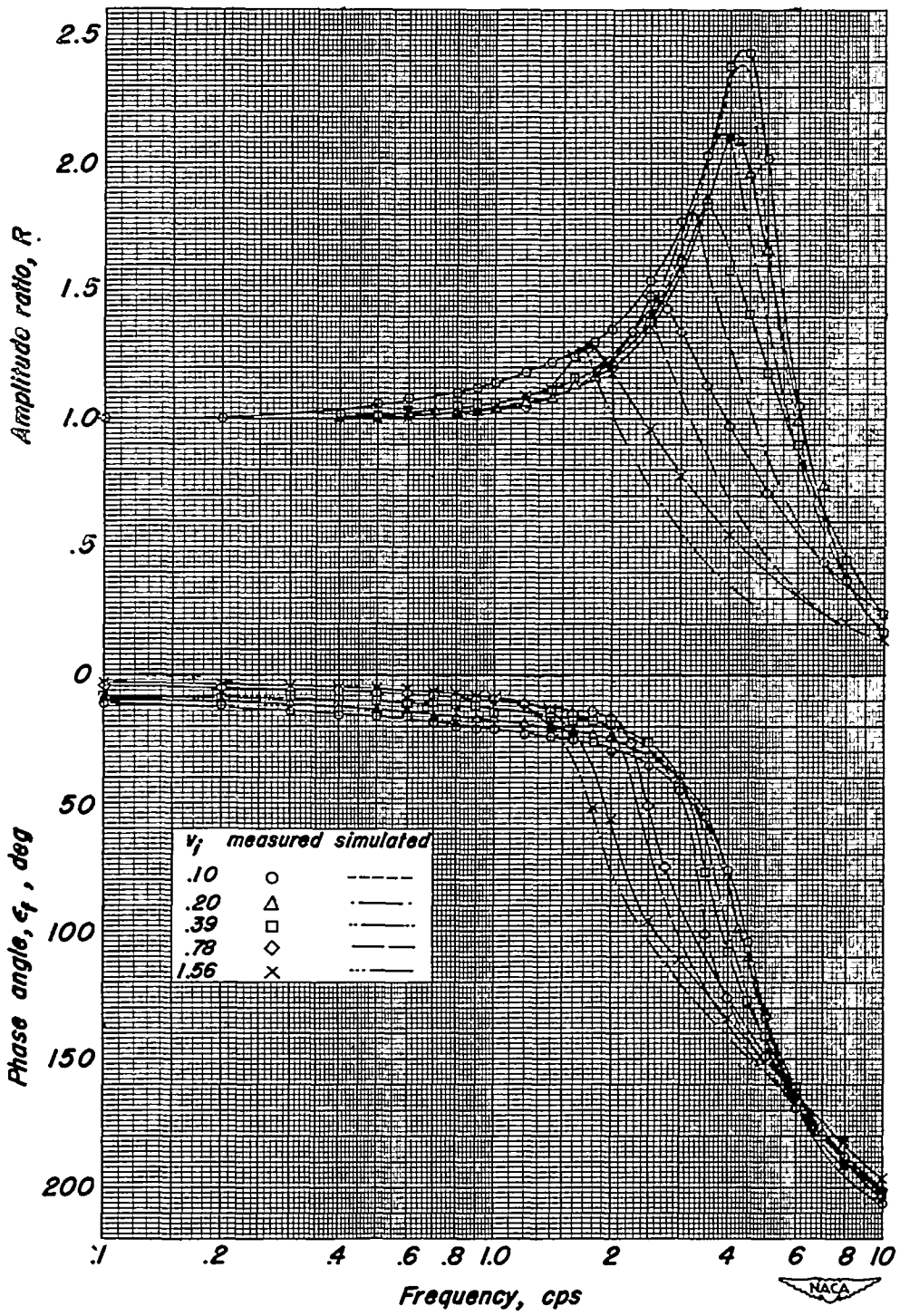

(b) $P_f = 0.42$

Figure 3.- Continued.

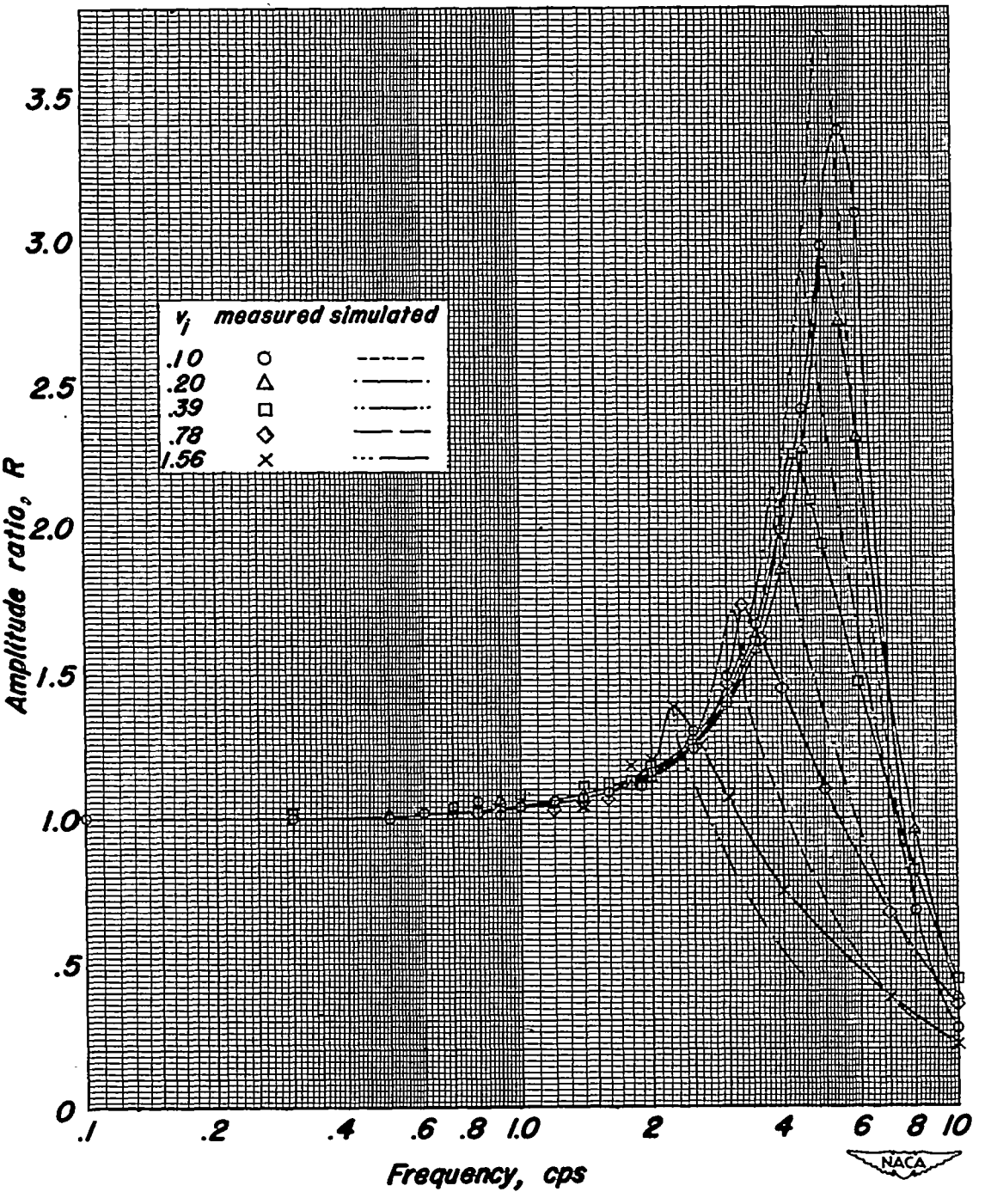

(c) Amplitude ratio, P_f=0.63.

Figure 3.- Continued.

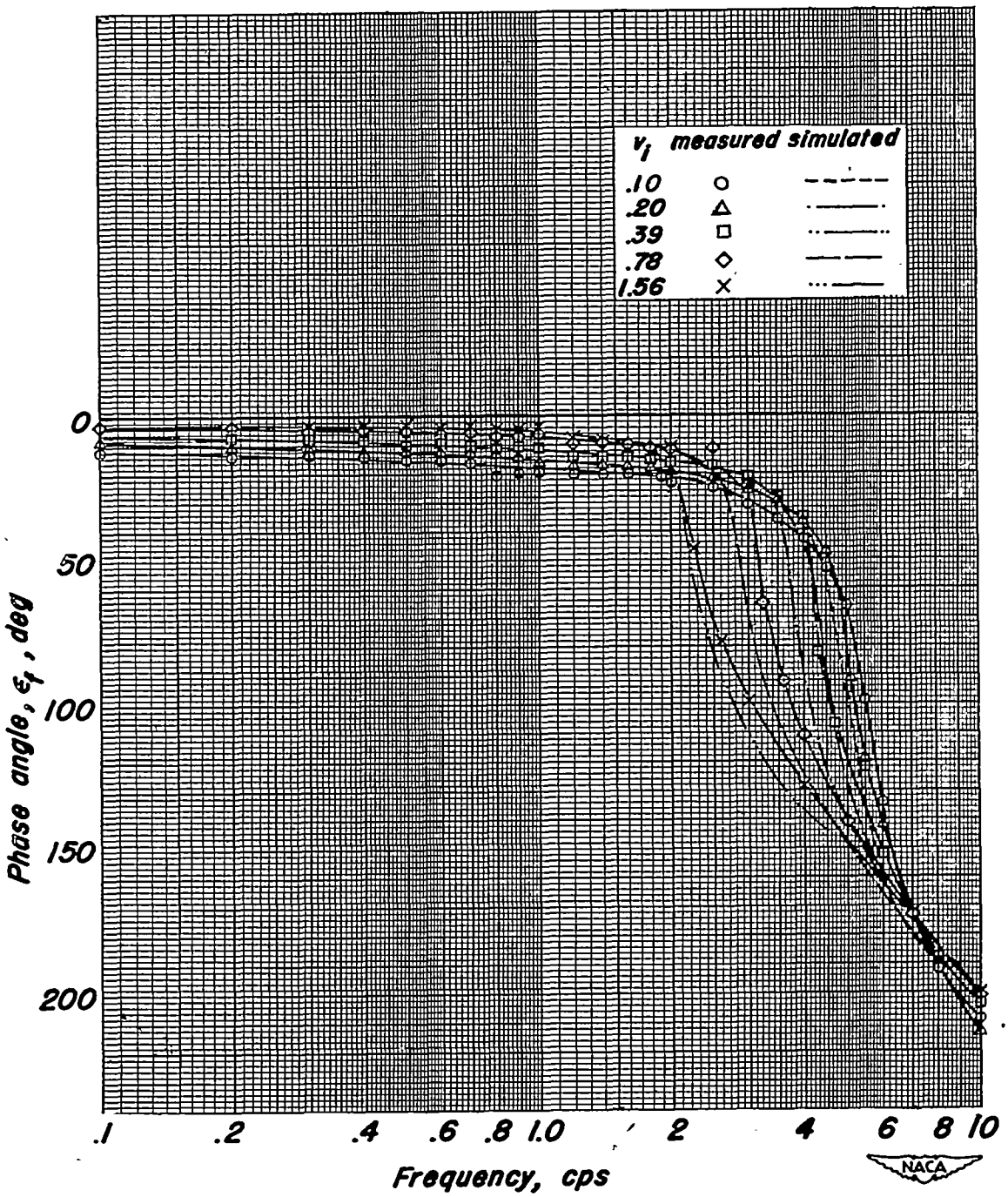

(d) Phase angle, $P_f = 0.63$.

Figure 3.- Continued.

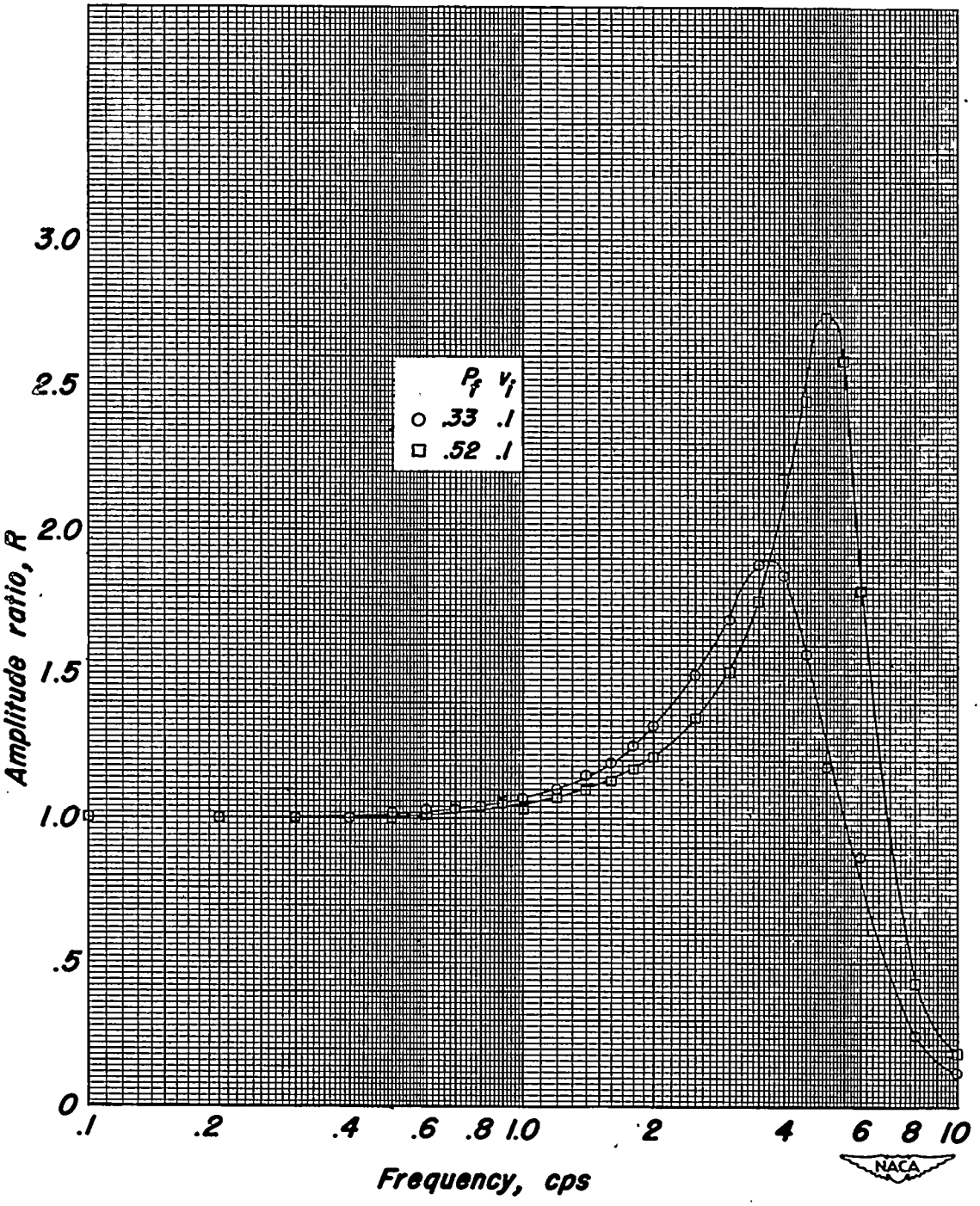

(e) Measured amplitude ratio, P_f = 0.33, 0.52.

Figure 3.- Continued.

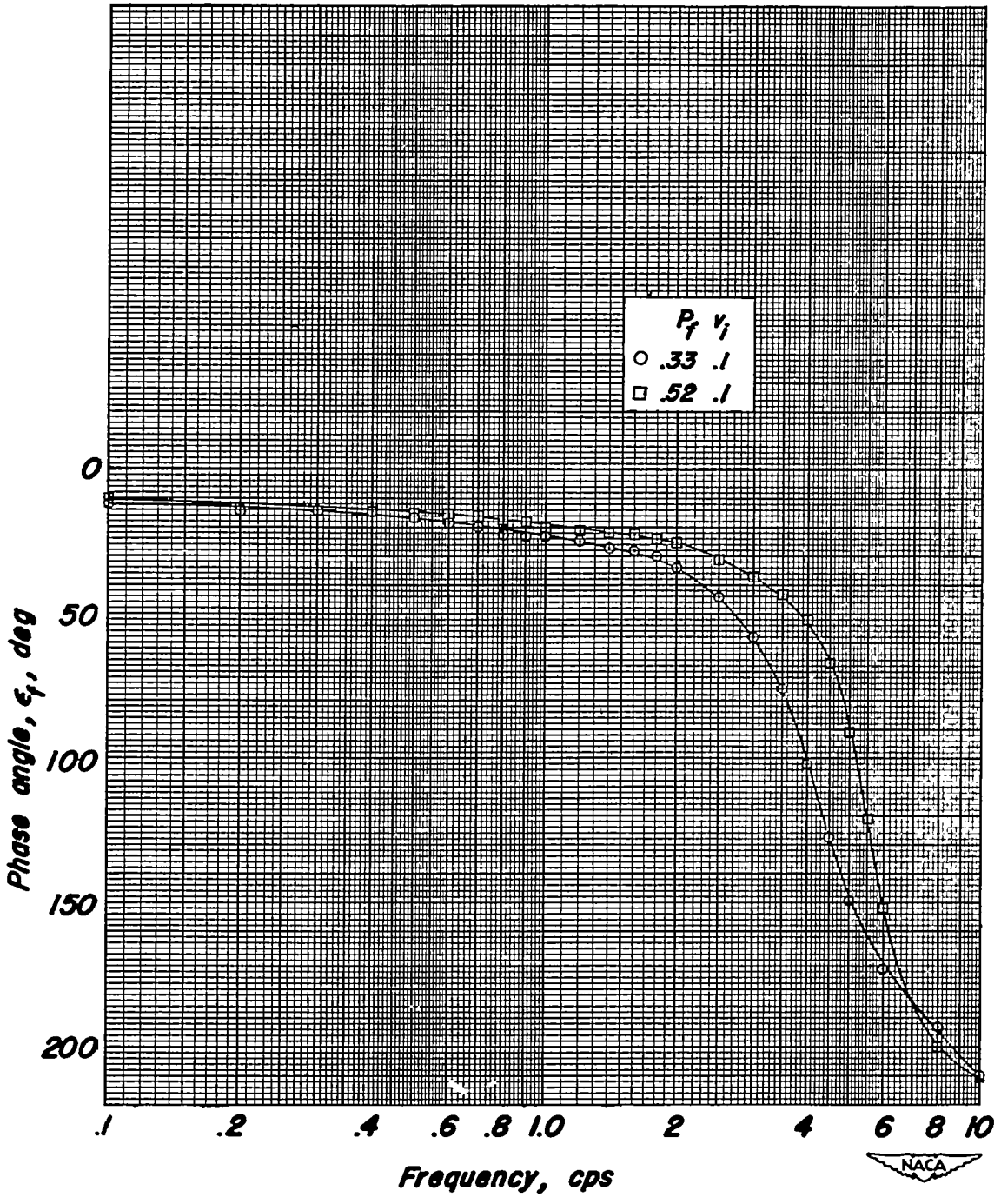

(f) Measured phase angle, P_f=0.33, 0.52.

Figure 3.- Concluded.

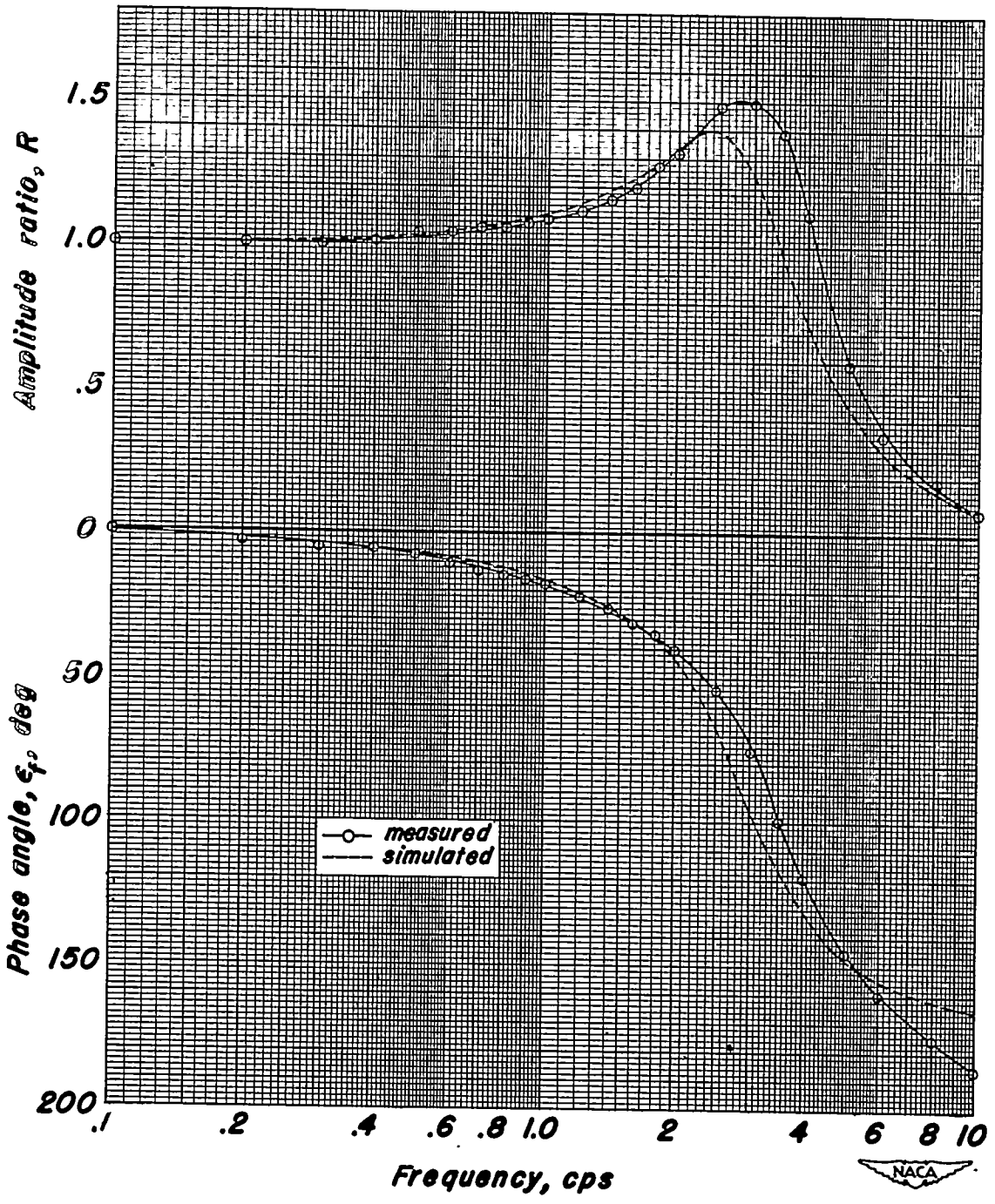

Figure 4.- Comparison of measured closed-loop frequency response of servo system and simulated response without time lags. P_f=0.24, v_i=0.1 . For simulation k_m=0.063, τ_m=0.071 .

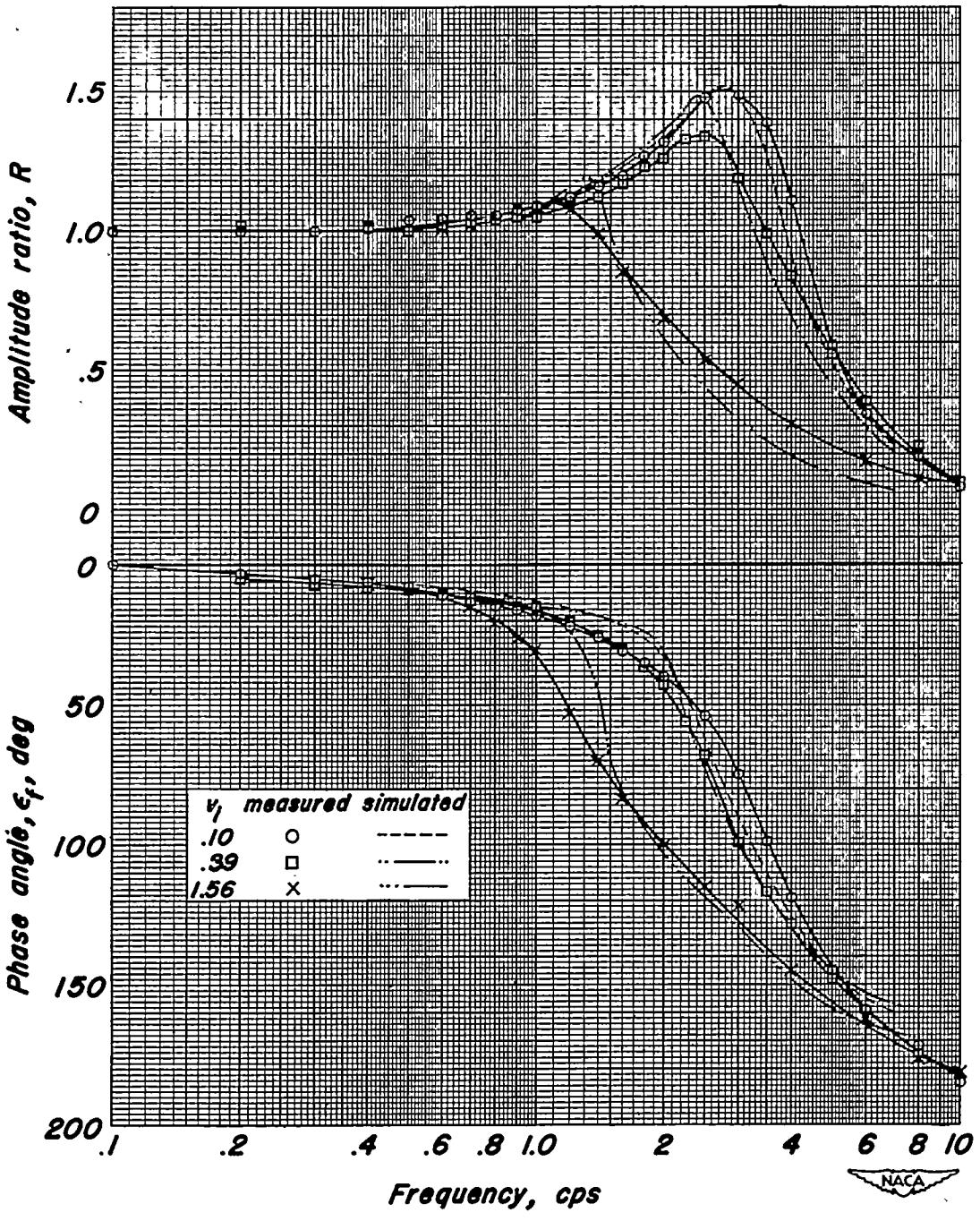

Figure 5.- Comparison of measured closed-loop frequency response of servo system and simulated response without time lags. P_f=0.24 . For simulation k_m=0.076, τ_m=0.071 .

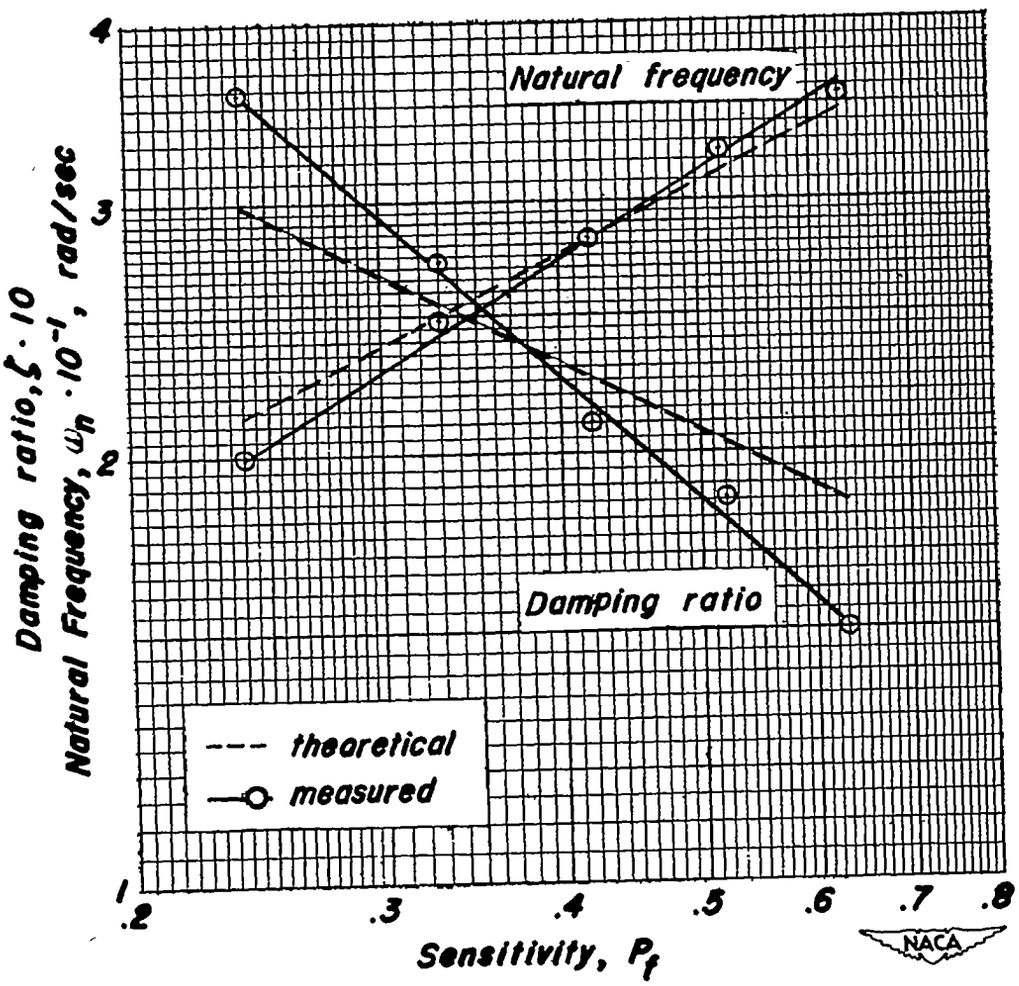

Figure 6.- Variation of damping ratio and natural frequency of servo system with feedback sensitivity on logarithmic coordinates.

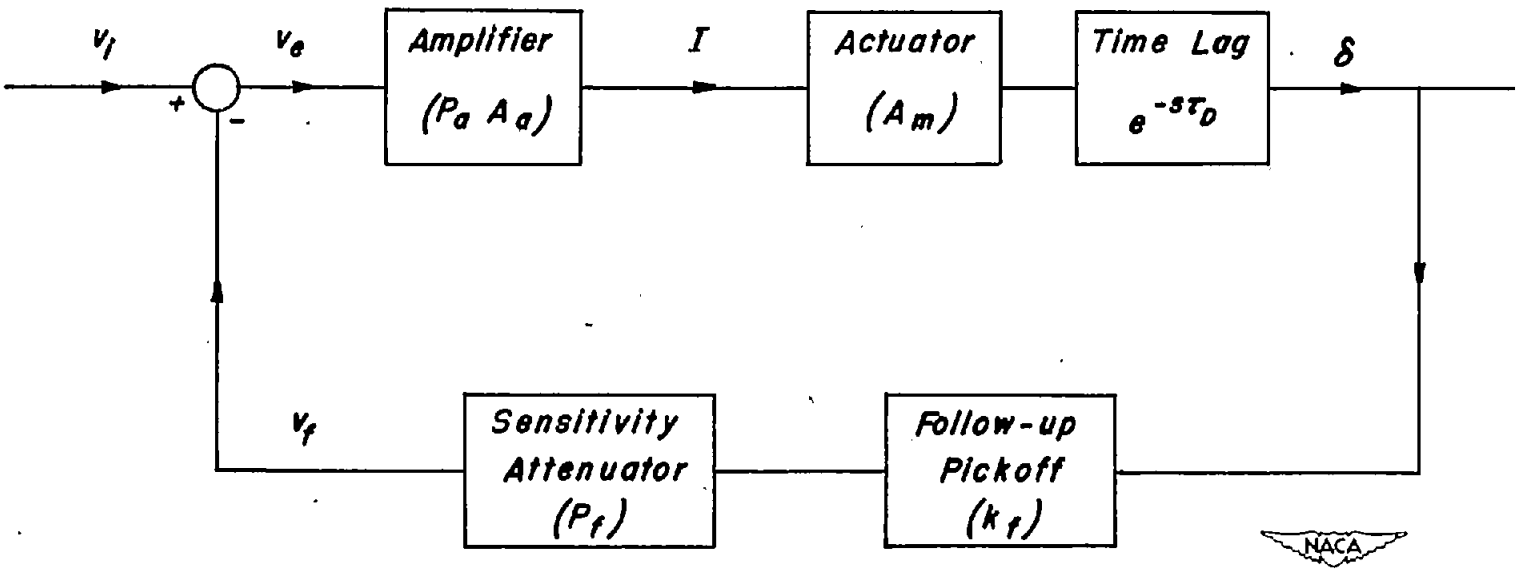

Figure 7.- Revised block diagram of servo-system loop.

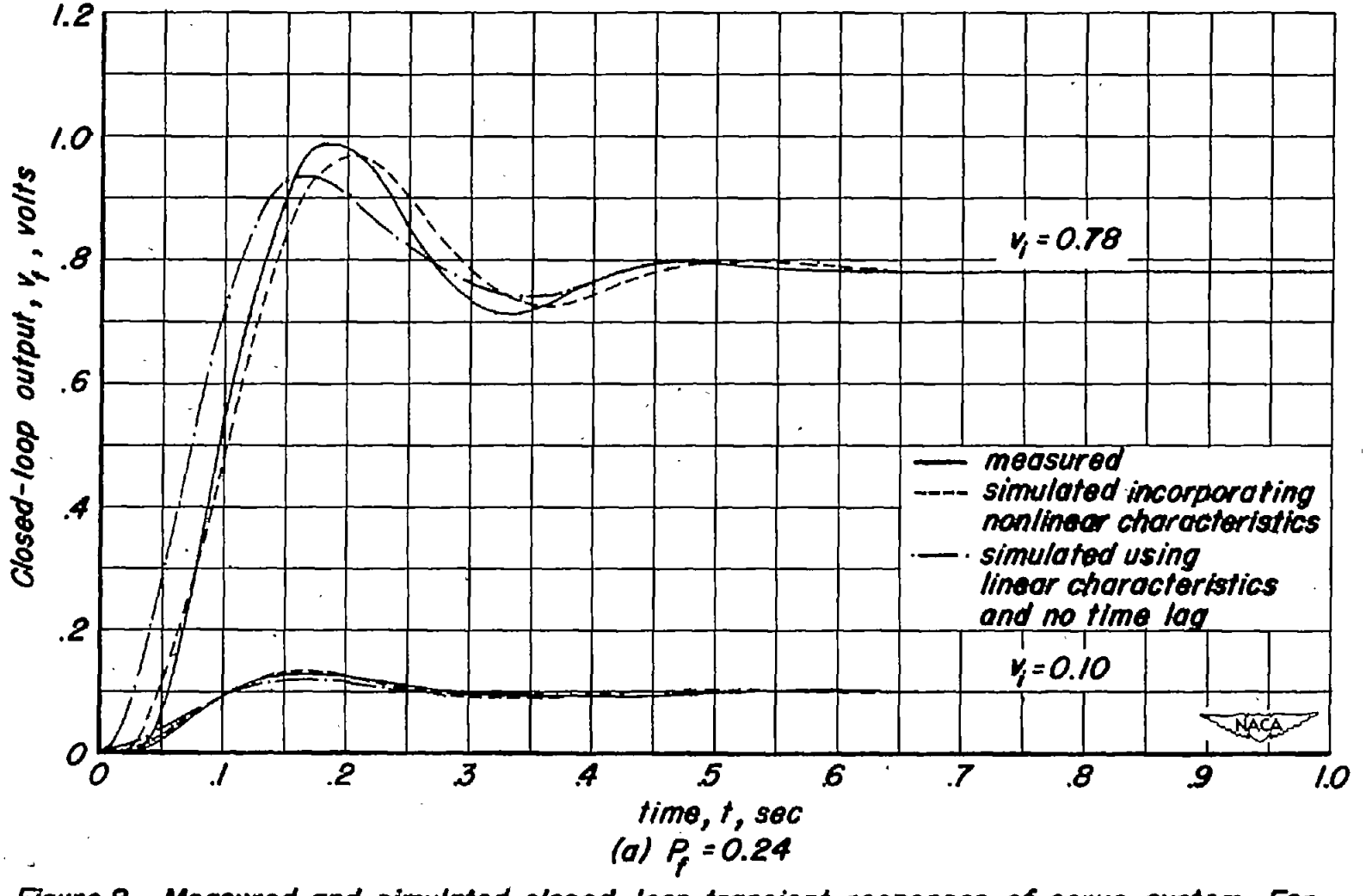

(a) $P_f = 0.24$

Figure 8.- Measured and simulated closed-loop transient responses of servo system. For simulation $k_f = 12.8$, $k_m = 0.063$, $\tau_m = 0.052$, $\tau_D = 0.009$.

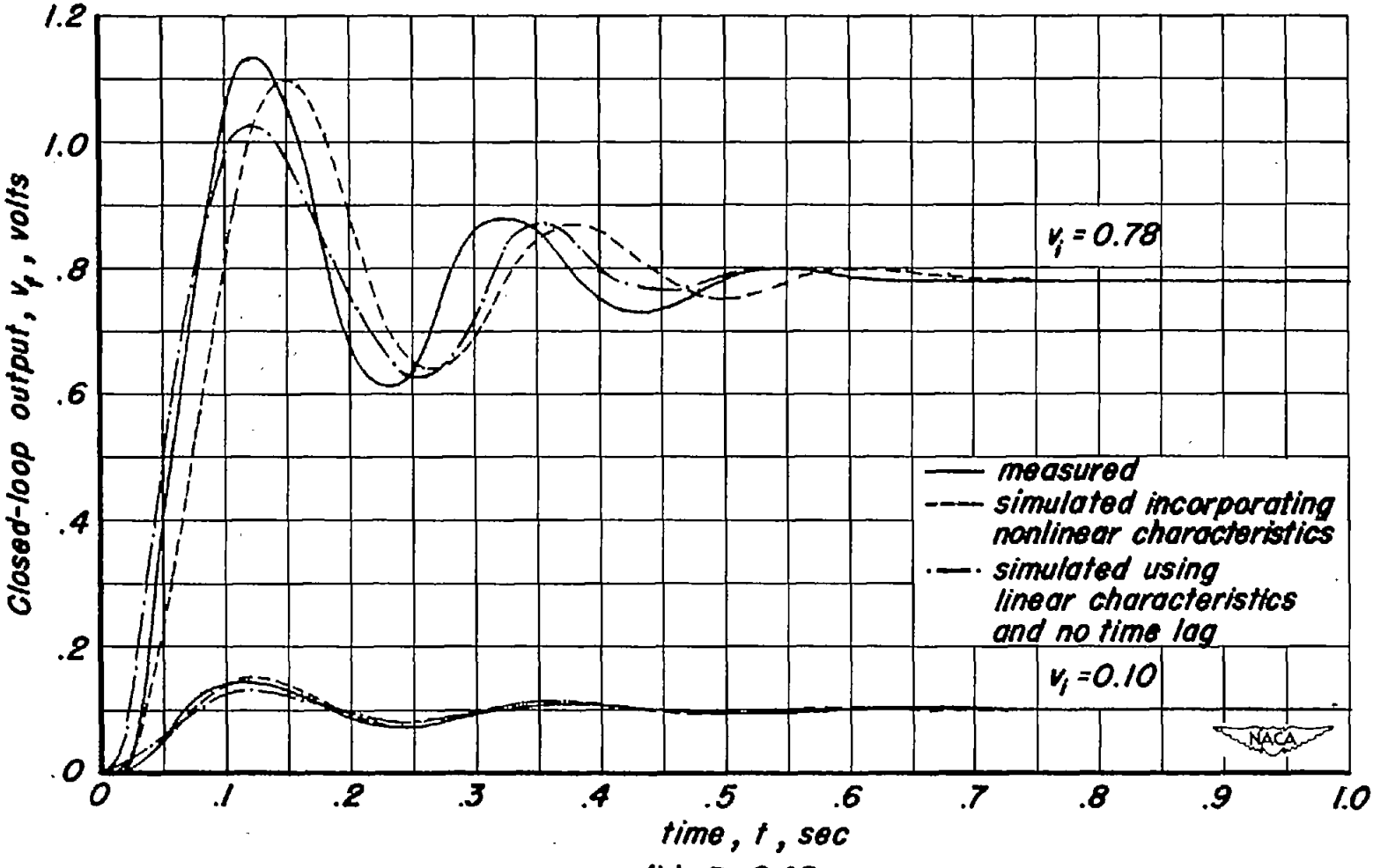

(b) P_f=0.42

Figure 8.- Continued.

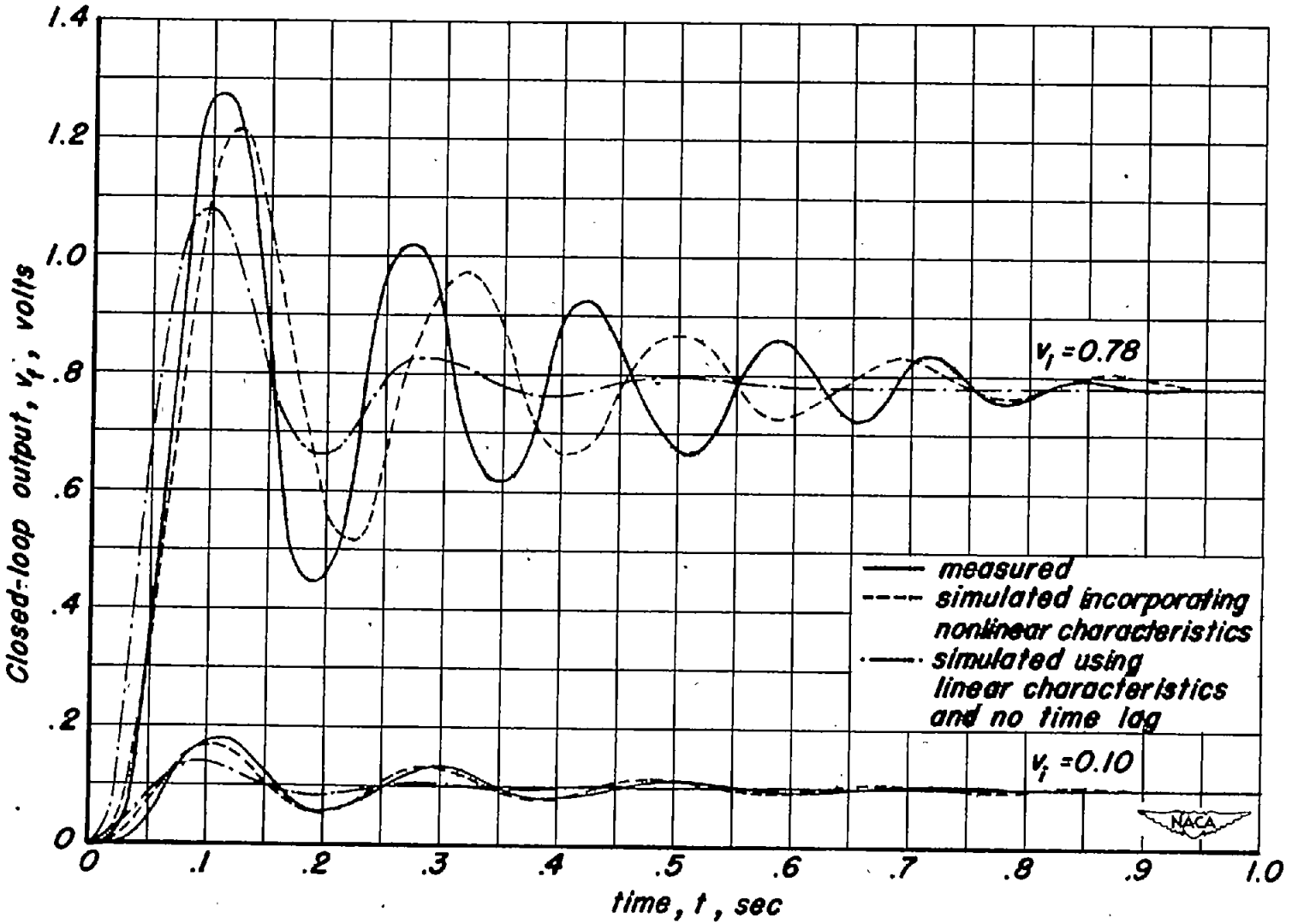

(c) P_f = 0.63

Figure 8.- Concluded.

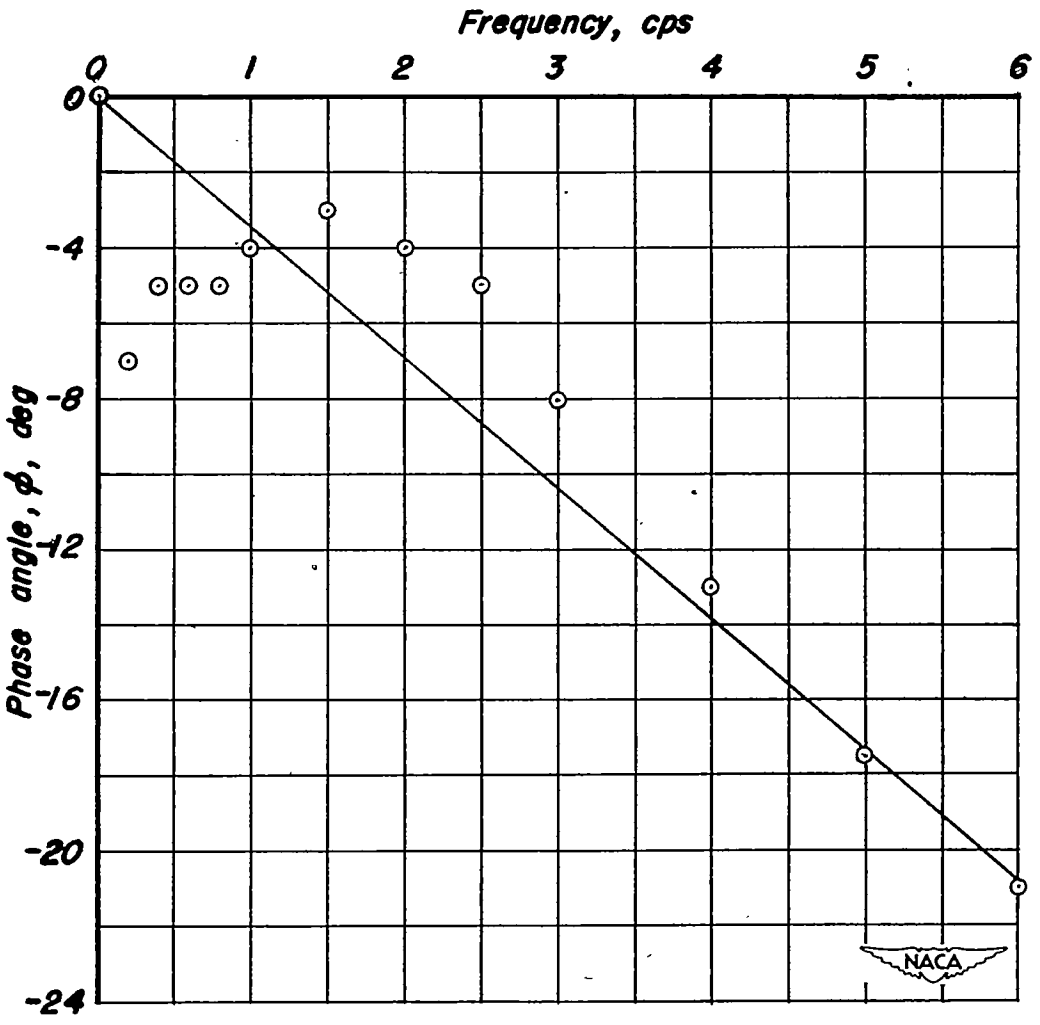

Figure 9.- Difference in phase angles between measured servo-system open-loop response and second-order term $1/s(1+\tau_m s)$.

NACA-Langley - 6-3-52 - 1000